Pergamon

Int. J. Heat Mass Transfer. Vol. 40, No. 6, pp. 1447–1458, 1997

0017–9310/97 $17.00+0.00

PII: S0017-9310(96)00172-X

Effects of Coriolis force and surface tension on Bénard–Marangoni convective instability

JONG JHY JOU, KUANG YUAN KUNG and CHENG HSING HSU

Department of Applied Mathematics, Feng Chia University, Taichung, Taiwan 40724, Republic of China, Department of Mechanical Engineering, Chung Yung University, Chung Li, Taiwan 32054, Republic of China

(*Received* 7 *November* 1995 *and in final form* 6 *May* 1996)

Abstract—The effect of the Coriolis force on the onset of the Bénard–Marangoni convective instability in a horizontal fluid layer, subject to a rotation, is investigated. The upper surface is deformably free and the lower surface is bounded with a solid plate, heated from below. The principle of exchange of stability is applied. The characteristic problem is solved numerically, using the Runge–Kutta–Gill's shooting method. The numerical results obtained compared very well with previously published ones. The thickness ratio d_r, conductivity ratio k_r, Biot number Bi, Crispation number C and Taylor number Ta are significant on determining the critical Rayleigh number R_c or Marangoni number M_c with the corresponding critical wavenumber a_c. The results show that the system is more stabilizing at larger values of the thickness ratio d_r, conductivity ratio k_r, Biot number Bi and Taylor number Ta. Copyright © 1996 Elsevier Science Ltd.

INTRODUCTION

The occurrence of cellular convection in a fluid layer, bounded with a deformably free upper surface and a lower rigid surface and subject to various thermal conditions, displays two instability mechanisms. The Rayleigh–Bénard convective instability is caused by a vertically unstable density stratification. While the Marangoni instability, as a result of the local variation of the interfacial tension with the temperature, was first analyzed by Pearson [1]. Efforts have been made in finding a mechanism for suppressing or augmenting convection in material science processing, especially the low-gravity melt processing and crystal growth processing in an orbiting space craft, such that the manufactured materials are free from impurities. The important effects involved are the surface tension, crystal-line anisotropy, nonequilibrium solidification and convection. Applications of the Bénard–Marangoni convection can be found in oil extraction from a porous medium, energy storage in molten salts and surface chemical reactions.

Geophysically, non-uniform heating is imparted by the sun onto the oceanic and continental surfaces, as well as the atmosphere, from above. The key mechanisms are the deformability of the free surface, the non-uniform heating and the rotation of the earth. The Bénard problem has been intensively studied with or without the rotation [2–6]. The stabilizing effect of the Coriolis force has already been demonstrated for the slow flow motion driven by the thermal buoyancy [3].

The Marangoni instability without rotation has been analyzed theoretically [7–9] and experimentally [10–11]. Several investigators have studied the surface-tension driven instability with rotation. In investigating the Marangoni instability, Vidal and Acrivos [12] and McConaghy and Finlayson [13] neglected the thermal buoyancy and assumed surface deformation. Friedrich and Rudraiah [14] considered a non-uniform temperature gradient and showed the stabilizing effect of the Taylor number. The Coriolis force and the parabolic temperature profile are suitable for material processing in a microgravity environment, because of the suppressing effects. Kaddame and Lebon [15] examined a more general problem of the coupled Bénard–Marangoni convective instability in a rotating fluid with a upper surface deflection. The Coriolis force, resulting from the rotation, suppresses Bénard–Marangoni convective instability [12–15], since the produced vertical shear dissipates some potential energy of the thermal buoyancy.

Nield [16] investigated the Bénard–Marangoni instability in a system, consisting of a horizontal fluid layer overlaying a porous medium layer and being subject to a uniform heating from below. A perturbation expansion in terms of a small wavenumber is applied to obtain a set of simple analytic solutions. Yang [17], who replaced the porous medium layer with a solid plate, found the stabilizing effects of the solid plate with the larger thermal conductivity and thickness ratios and clarified some features of the parallel flow assumption, suitable for smaller values of the product of the thickness and conductivity ratios. As studied previously, the bottom surface is imposed with a uniform heat flux or an isothermal temperature, Yang [17] recommended a Neumann type condition in the form $\nabla T \cdot \hat{n} = Bi\, T$, which may very well rep-

NOMENCLATURE

a	wavenumber
Bi	Biot number, qd_l/k_l
Bo	Bond number, $Bo = \rho g d_l^2/\gamma_0$
C	Crispation number, $C = \mu D_f/\gamma_0 d_l$
d_l	horizontal average of thickness of fluid layer
d_r	depth ratio, d_s/d_l
d_s	thickness of solid plate
D_f	thermal diffusivity of liquid layer
D_s	thermal diffusivity of solid plate
g	gravity
h	dimensionless form of h_l
h_l	position of the deformability free upper surface about d_l
k_l	thermal conductivity of fluid layer
k_r	conductivity ratio, k_s/k_l
k_s	thermal conductivity of solid plate
M	Marangoni number, $-\partial\gamma(T_0)/\partial T_l \cdot \Delta T_l/\mu D_f$
Pr	Prandtl number, ν/D_f
q	heat transfer coefficient
R	Rayleigh number, $\alpha g \Delta T_l a_l^3/\nu D_f$
t	time
T_l	temperature of fluid
T_s	temperature of solid plate
T_0	ambient temperature
Ta	Taylor number, $4\Omega^2 d_l^4/\nu^2$
w	dimensionless velocity in z direction
W	normal mode of w
x, y, z	Cartesian coordinates
Z	normal mode of h.

Greek symbols

α	coefficient of thermal expansion of fluid density
γ	surface tension
γ_0	surface tension at T_0, $\gamma(T_0)$
ΔT_l	temperature difference across the liquid layer
ζ	dimensionless perturbed velocity in z direction
Θ_l	normal mode of θ_l
Θ_s	normal mode of θ_s
θ_l	dimensionless perturbed temperature of fluid
θ_s	dimensionless perturbed temperature of solid plate
μ	dynamic viscosity of fluid
ν	kinematic viscosity of fluid
ξ	normal mode of ζ
ρ	density of fluid
ρ_0	density of fluid at T_0
τ	negative rate of change of the surface tension at T_0, $\tau = -\partial\gamma(T_0)/\partial T_l$
ω	growth parameter
Ω	frequency of rotation.

Subscripts

c	critical scale
l	liquid property
r	ratio of liquid property to solid property
s	solid property.

resent the general situation in the practical experiments [10–11], especially when dealing with a solid layer of finite thickness.

The present study concentrates on the effects of the thickness ratio d_r, conductivity ratio k_r, Biot number Bi, Crispation number C and Taylor number Ta on the Bénard–Marangoni convective instability. The parallel flow assumption has been derived for wide ranges of the physical parameters [16–19]. This shooting technique, avoiding the complicated mathematical procedure and being easily applied to solve the generalized problem with the excellent accuracy, is shown to be more effective than the power method [3] and the energy method [8].

PHYSICAL FORMULATION

A horizontal fluid layer, open to the ambient air, with thickness $d_l + h_l(x, y, t)$ and thermal conductivity k_l is considered; where d_l is the horizontal average of the thickness of the fluid layer and $h_l(x, y, t)$ is the position of the deformably free upper surface about d_l. The lower surface is bounded by a solid plate with thickness d_s and thermal conductivity k_s. The solid plate is subjected to a fixed heat flux from below. For the fluid layer the Boussinesq approximation is assumed (except for the surface tension) to be varying with the temperature. The equation of state is

$$\rho = \rho_0[1 - \alpha(T_l - T_0)] \tag{1}$$

where ρ is the density, T_l is the temperature of the fluid, α is the coefficient of thermal expansion and ρ_0 is the fluid density at the ambient temperature T_0.

Adopting a set of scales $[d_l, d_l^2/D_f, D_f/d_l, D_f/d_l^2, \Delta T_l]$ for length, time, velocity, vorticity and temperature, respectively, where D_f is the thermal diffusivity, then the linearized governing equations of the perturbed state in dimensionless forms are

$$\frac{1}{Pr}\frac{\partial \zeta}{\partial t} = \nabla^2 \zeta + \sqrt{Ta}\frac{\partial w}{\partial z} \tag{2}$$

$$\frac{1}{Pr}\frac{\partial}{\partial t}\nabla^2 w = R\nabla_H^2 \theta_l + \nabla^4 w - \sqrt{Ta}\frac{\partial \zeta}{\partial z} \tag{3}$$

$$\frac{\partial \theta_l}{\partial t} = w + \nabla^2 \theta_l \tag{4}$$

where w, θ_l and ζ are the z axis components of the velocity, the temperature and the vorticity perturbations in dimensionless forms respectively. The Prandtl number Pr, the Rayleigh number R and the Taylor number Ta are defined as

$$Pr = \nu/D_f,\ R = \alpha g\, \Delta T_l d_l^3/\nu D_f,\ Ta = 4\Omega^2 d_l^4/\nu^2. \tag{5}$$

∇_H^2 is the horizontal Laplacian operator

$$\nabla_H^2 = \partial^2/\partial x^2 + \partial^2/\partial y^2. \tag{6}$$

For the solid plate, the linearized governing equation of the perturbed state in the dimensionless form is

$$\frac{\partial \theta_s}{\partial t} = D_s/D_f \nabla^2 \theta_s. \tag{7}$$

The surface tension γ is assumed to vary linearly with the temperature,

$$\gamma = \gamma_0 - \tau(T_l - T_0). \tag{8}$$

where $\gamma_0 = \gamma(T_0)$ is the surface tension at T_0 and $\tau = -\partial\gamma(T_0)/\partial T_l$ is the negative rate of change of the surface tension at T_0.

At the deformably free upper surface, at $z = 1 + h(x, y, t)$, balances of heat, normal and shear stresses are required. Expanding the variables about $z = 1$ the boundary conditions of the upper surface are reduced to

$$\frac{\partial h}{\partial t} = w \tag{9}$$

$$\left(\frac{\partial}{\partial z} + Bi\right)\theta_l - Bi\, h = 0 \tag{10}$$

$$C\left[\left(-\frac{1}{Pr}\frac{\partial}{\partial t} + 3\nabla_H^2 + \frac{\partial^2}{\partial z^2}\right)\frac{\partial w}{\partial z} - \sqrt{Ta}\,\zeta\right] + (B_o - \nabla_H^2)\nabla_H^2 h = 0 \tag{11}$$

$$\left(\frac{\partial^2}{\partial z^2} - \nabla_H^2\right)w + M\nabla_H^2(h - \theta_l) = 0 \tag{12}$$

$$\frac{\partial \zeta}{\partial z} = 0 \tag{13}$$

where the Crispation number C and the Marangoni number M are defined as

$$C = \frac{\mu D_f}{\gamma_0 d_l} \tag{14}$$

$$M = -\frac{\partial\gamma(T_0)}{\partial T_l}\frac{\Delta T_l}{\mu D_f} d_l \tag{15}$$

and $Bo = \rho g d_l^2/\gamma_0$ is the Bond number which is a measure of the flattening of the surface by gravity with that due to the surface tension, and $Bi = q d_l/k_l$ is the Biot number. At the solid–liquid interface, at $z = 0$, the non-slip conditions and thermal boundary conditions are

$$w = \partial w/\partial z = \zeta = 0 \tag{16}$$

$$\theta_l = \theta_s,\ k_l\, \partial\theta_l/\partial z = k_s\, \partial\theta_s/\partial z. \tag{17}$$

At the bottom surface, at $z = -d_s/d_l$, a uniform heat flux is imposed,

$$\partial\theta_s/\partial z = 0. \tag{18}$$

The perturbed quantities in terms of normal modes are

$$\begin{bmatrix} w \\ \theta_l \\ \theta_s \\ \zeta \\ h \end{bmatrix} = \begin{bmatrix} W(z) \\ \Theta_l(z) \\ \Theta_s(z) \\ \xi(z) \\ Z \end{bmatrix} \exp\left[i(a_x x + a_y y) + \omega t\right] \tag{19}$$

where $a = (a_x^2 + a_y^2)^{1/2}$ is the dimensionless wavenumber of disturbances and ω is the growth parameter, which in general is complex. By substituting equation (19) into equations (2)–(4) and (7), we obtain

$$\left(D^2 - a^2 - \frac{\omega}{Pr}\right)\xi + \sqrt{Ta}\, DW = 0 \tag{20}$$

$$\left(D^2 - a^2 - \frac{\omega}{Pr}\right)(D^2 - a^2)W - Ra^2\Theta_l - \sqrt{Ta}\, D\xi = 0 \tag{21}$$

$$(D^2 - a^2 - \omega)\Theta_l + W = 0 \tag{22}$$

$$\left(D^2 - a^2 - \frac{D_f}{D_s}\omega\right)\Theta_s = 0 \tag{23}$$

where the operator $D = \partial/\partial z$. The boundary conditions at $z = 1$ are

$$\omega Z = W \tag{24}$$

$$(D + Bi)\Theta_l - BiZ = 0 \tag{25}$$

$$C\left[\left(D^2 - 3a^2 - \frac{\omega}{Pr}\right)DW - \sqrt{Ta}\,\xi\right] - (B_o + a^2)a^2 Z = 0 \tag{26}$$

$$(D^2 + a^2)W - Ma^2(Z - \Theta_l) = 0 \tag{27}$$

$$D\xi = 0. \tag{28}$$

The boundary conditions at $z = 0$ are

$$W = DW = \xi = 0 \tag{29}$$

$$\Theta_l = \Theta_s,\ D\Theta_l = k_r D\Theta_s \tag{30}$$

where $k_r = k_s/k_l$ is the conductivity ratio.

The boundary condition at $z = -d_r$, where $d_r = d_s/d_l$ is the thickness ratio, is

$$D\Theta_s = 0. \tag{31}$$

NUMERICAL CALCULATIONS

The problem is complex mathematically and the analytical solutions are impractical to obtain, except for simplified cases studied by Pellow and Southwell [2], Chandrasekhar [3], Nield [16] and Yang [17–19]. The principle of exchange of stability has been proven to be valid for the Bénard problem [2] and for the case with rotation at sufficiently large values of the Prandtl number Pr [3]. For Marangoni convective instabilities with a flat free surface, it also held for a non-rotating fluid by Vidal and Acrivos [20] and for a rotating fluid with higher values of the Prandtl number Pr by McConaghy and Finlayson [13]. We deal with higher values of the Prandtl number Pr and assume a flat free surface (i.e. $C = 0$) such that overstabilities may be neglected and, following the previous studies [7, 15–17], set $\omega = 0$ for the neutral stability. Also, the effect of the Bond number Bo can be incorporated into that of the surface tension, as illustrated in equation (26). We may set $Bo = 0.1$ everywhere.

The governing equations of the perturbed state, which are composed of ordinary differential equations of order eight in the fluid-layer and of order two in the solid layer, include equations (20)–(22) and (23) and are subject to boundary conditions (24)–(31). A Sturm–Liouville's problem is formed, with the Rayleigh number R or the Marangoni number M, being the eigenvalue, while keeping other physical parameters Bi, d_r, k_r, Ta and a fixed. The computational procedure through the Runge–Kutta–Gill's shooting method is applied to fit the required boundary conditions. For a non-trivial solution of the system to exist, it is required to extract the eigenvalue from the following characteristic equation,

$$f(R, M, a, Bi, d_r, k_r, Ta) = 0. \tag{32}$$

The minimum eigenvalue with the corresponding wavenumber gives rise to the critical condition $[R_c, a_c]$ or $[M_c, a_c]$, marking the marginal state. The computational procedure is given below. For the fluid layer, we let

$$W = u_1$$

$$DW = Du_1 = u_2 \tag{33}$$

$$D^2W = Du_2 = u_3 \tag{34}$$

$$D^3W = Du_3 = u_4 \tag{35}$$

$$D^4W = Du_4 = 2a^2u_3 - a^4u_1 + Ra^2u_5 + \sqrt{Ta}\,u_8 \tag{36}$$

$$\Theta_1 = u_5$$

$$D\Theta_1 = Du_5 = u_6 \tag{37}$$

$$D^2\Theta_1 = Du_6 = a^2u_5 - u_1 \tag{38}$$

$$\xi = u_7$$

$$D\xi = Du_7 = u_8 \tag{39}$$

$$D^2\xi = Du_8 = a^2u_7 - \sqrt{Ta}\,u_2. \tag{40}$$

Equation (23) of the solid layer is solved such that the relation for the temperature of the fluid layer is achieved, then the boundary conditions (29)–(30) at the solid–liquid interface at $z = 0$ turn into the following forms,

$$u_1 = 0 \tag{41}$$

$$u_2 = 0 \tag{42}$$

$$u_6 = k_r a \tanh(ad_r)u_5 \tag{43}$$

$$u_7 = 0 \tag{44}$$

we guessed four more boundary conditions by choosing

$$u_3 = b_1,\ u_4 = b_2,\ u_5 = b_3,\ u_8 = b_4 \tag{45}$$

then, we had

$$\mathbf{U} = b_1\mathbf{U}_1 + b_2\mathbf{U}_2 + b_3\mathbf{U}_3 + b_4\mathbf{U}_4 \tag{46}$$

where

$$\mathbf{U}_1 = [0,0,1,0,0,0,0,0]^T$$

$$\mathbf{U}_2 = [0,0,0,1,0,0,0,0]^T$$

$$\mathbf{U}_3 = [0,0,0,0,1,k_r a\tanh(ad_r),0,0]^T$$

$$\mathbf{U}_4 = [0,0,0,0,0,0,0,1]^T.$$

We guessed an initial value for R or M, using the Runge–Kutta–Gill's shooting method, starting from $z = 0$ and tried to match the boundary conditions at $z = 1$, then, a matrix system was obtained,

$$\mathbf{MB} = 0$$

where

$$\mathbf{M} = [m_{ij}],\ \mathbf{B} = [b_j]\ i,j = 1,4$$

$$m_{1j} = \mathbf{U}_j^1$$

$$m_{2j} = \mathbf{U}_j^6 + Bi\mathbf{U}_j^5 - \frac{CBi}{a^2(B_o + a^2)}\mathbf{U}_j^4 + \frac{3CBi}{B_o + a^2}\mathbf{U}_j^2 + \frac{CBi\sqrt{Ta}}{a^2(B_o + a^2)}\mathbf{U}_j^7$$

$$m_{3j} = \mathbf{U}_j^3 - \frac{CM}{B_o + a^2}\mathbf{U}_j^4 + \frac{3CMa^2}{B_o + a^2}\mathbf{U}_j^2 + Ma^2\mathbf{U}_j^5 + \frac{CM\sqrt{Ta}}{B_o + a^2}\mathbf{U}_j^7$$

$$m_{4j} = \mathbf{U}_j^8$$

where $\mathbf{U}_j^i$ is the ith element of the jth vector $\mathbf{U}_j$. For a non-trivial solution of the matrix system to exist, the determinant of the matrix $\mathbf{M}$ should be zero and the approximate eigenvalue R or M was thus found.

RESULTS AND DISCUSSIONS

In order to validate the present solutions, some results are achieved and compared with previous studies. For a flat free upper surface, $M = 0$, without the rotation effect $Ta = 0$, for two limiting thermal conditions, uniform heat flux and constant temperature, at the lower surface, the critical conditions $[R_c, a_c]$ are [817.062, 2.215] and [1101.219, 2.683], respectively, provided the upper surface is fixed with a constant temperature (i.e., $Bi^{-1} = 0$). The comparable results are [816.748, 2.21] and [1100.657, 2.68] [4], while the critical conditions $[R_c, a_c]$ are [320.087, 0] and [669.235, 2.086], respectively, provided the upper surface is fixed with a uniform heat flux (i.e., $Bi = 0$). The comparable results are [320.000, 0] and [669.001, 2.09] [4]. The above trends are obviously shown in Fig. 1 and Fig. 2. For both parameters d_r and k_r to be either very small or very large, the limiting thermal conditions at the lower boundary are recovered. Yang [17] has shown the boundary effects on the Bénard–Marangoni convective instabilities and his results were in good agreement with previous works by Nield [7], Sparrow *et al.* [4] and Garcia *et al.* [21].

In considering the Rayleigh–Bénard convection, we may set $M = 0$. The critical Rayleigh number R_c is a function of the thickness ratio d_r, the thermal conductivity ratio k_r, the Taylor number Ta, the Bond number Bo and the Biot number Bi. Figure 1 shows the critical Rayleigh number R_c as a function of the thickness ratio d_r for various values of the thermal conductivity ratio k_r and, for the case of constant temperature at the upper surface with $Bi^{-1} = 0$ and $Ta = 0$ and 1000. The dashed-lines correspond to cases without rotation [17]. For small values of the thermal conductivity ratio k_r, the solid plate tends toward being adiabatic and the thermal energy of disturbances is efficiently transferred into the fluid layer through the fluid–solid interface, hence, a less stabilizing system is expected. For large values of the thermal conductivity ratio k_r, the solid plate tends toward being isothermal and much of the thermal energy of disturbances is absorbed and stored in the solid plate instead, hence, a more stabilizing system is found. The critical Rayleigh number R_c increases monotonically with the thermal conductivity ratio k_r. The main effect of the thickness ratio d_r concentrates on the relative thickness of the solid plate in storing the amount of the thermal energy of disturbances. Obviously, the thicker the solid plate, the more thermal energy it would store and the more stabilizing the fluid layer would be. The critical Rayleigh number R_c increases monotonically with the thickness ratio d_r. For both parameters d_r and k_r to be very small or both to be very large, the limiting thermal conditions, uniform heat flux and constant temperature at the lower boundary are recovered. For $d_r \leqslant 0.1$ or $d_r \geqslant 1$, the increasing of R_c with the thickness ratio d_r is insignificant, irrespective of the thermal conductivity ratio k_r. For $d_r \leqslant 0.1$ and $k_r \leqslant 1$ as well as $d_r \geqslant 1$ and $k_r \geqslant 10$, the increasing of R_c with the thermal conductivity ratio k_r becomes negligibly small. It is worth noting that R_c increases with d_r at first and then, when $d_r \geqslant 1$, approaches an invariant value, depending on k_r. Also shown in Fig. 1 are cases with $Ta = 1000$ and the critical conditions $[R_c, a_c]$ are [1585.309, 3.264] and [1882.049, 3.627], corresponding to the limiting thermal conditions, uniform heat flux and constant temperature, at the lower surface, respectively. For

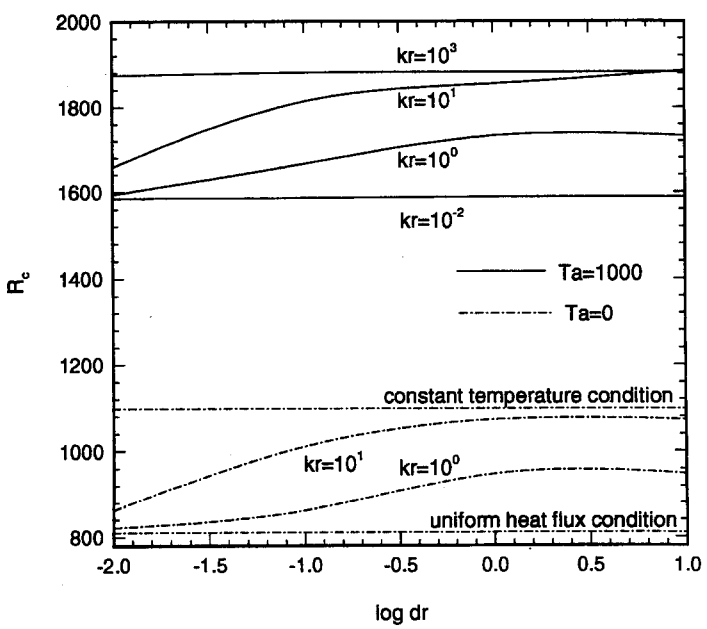

Fig. 1. The critical Rayleigh number R_c as a function of the thickness ratio d_r for various values of the thermal conductivity ratio k_r with $Bi^{-1} = 0$ and $Ta = 0$ and 1000.

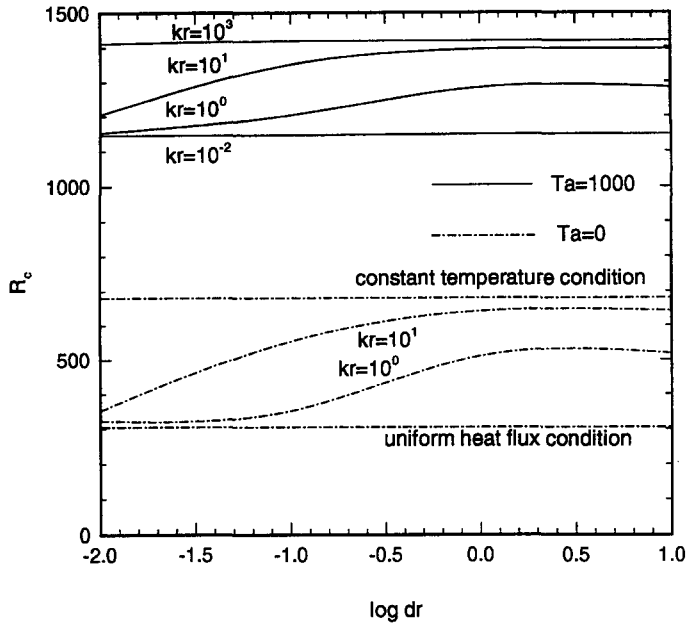

Fig. 2. The critical Rayleigh number R_c as a function of the thickness ratio d_r for various values of the thermal conductivity ratio k_r with $Bi = 0$ and $Ta = 0$ and 1000.

$Ta = 6.25 \times 10^3$, $Bo = 0$, the critical condition $[R_c, a_c]$ is [4047.7, 4.925] [3], comparable to [4045.5, 4.933] for this study, provided the lower surface is fixed at constant temperature. The stabilizing effect of the rotation would greatly raise the critical Rayleigh number R_c, while keeping the influence of the thickness ratio d_r and the thermal conductivity ratio k_r as discussed previously. Figure 2 shows the critical Rayleigh number R_c as a function of the thickness ratio d_r for various values of the thermal conductivity ratio k_r and for the case of constant heat flux at the upper surface with $Bi = 0$ and $Ta = 0$ and 1000. The physical discussions are quite similar to those for the case of constant temperature at the upper surface with $Bi^{-1} = 0$. In general, as a result of the thermal condition, the critical Rayleigh number R_c for the case of constant heat flux at the upper surface with $Bi = 0$ is much smaller than that for the case of constant temperature at the upper surface with $Bi^{-1} = 0$, irrespective of the Taylor number Ta. Usually, the latter case gives rise to a more destabilizing state [4, 7]. For $Ta = 1000$, the critical conditions $[R_c, a_c]$ are [1145.306, 2.539] and [1419.067, 3.147], corresponding to the limiting thermal conditions, uniform heat flux and constant temperature, at the lower surface, respectively.

The Rayleigh–Bénard convection without the surface tension effect is considered. Figure 3 shows the critical Rayleigh number R_c and wavenumber a_c as functions of the Taylor number Ta for various values of the thermal conductivity ratio k_r and for the case of constant heat flux at the upper surface with $Bi = 0$ and $d_r = 10$ and $M = 0$. It is obvious that the effect of the Coriolis force would suppress the onset of convection and the critical Rayleigh number R_c increases with the Taylor number Ta. For small values of the Taylor number, such as $Ta \leqslant 10^3$, the effect of the Coriolis force is insignificant. While, for $Ta \geqslant 10^4$, a rapid increase of the critical Rayleigh number R_c with the Taylor number Ta is shown. As $Ta \to \infty$, the Rayleigh–Bénard convection ceases to exist and the corresponding critical Rayleigh number R_c becomes infinite. Throughout the entire interval of the Taylor number, the effect of the thermal conductivity ratio k_r on the critical Rayleigh number R_c is small, because of the comparably finite thickness of the solid layer chosen for this case (i.e. $d_r = 10$). The same increasing trend of the critical wavenumber a_c with the Taylor number Ta is found, except that the effect of the thermal conductivity ratio k_r displays obvious variations with small values of the Taylor number Ta compared to large values. The parallel flow is possible only when the Taylor number Ta is very small and the thermal conductivity ratio k_r is tiny. For $Ta = 0$, a vanishing critical wavenumber with R_c being 320, is presented for the parallel flow [17]. Figure 3 also shows that the valid range of the Taylor number Ta for the parallel flow is, for $k_r = 10^{-4}$, about 0–10.

Figure 4 shows the critical Rayleigh number R_c and wavenumber a_c as functions of the Taylor number Ta for various values of the thermal conductivity ratio k_r and for the case of constant temperature at the upper surface with $Bi^{-1} = 0$ and $d_r = 10$ and $M = 0$. Special cases with constant temperature conditions at the upper surface and the lower fluid–solid boundary, by choosing $Bi^{-1} = 0$ and $k_r = 10^2$, compared very well with previous works [3]. The physical characteristics are similar between Fig. 3 and Fig. 4, except that the critical Rayleigh number and wavenumber in Fig. 4 are higher than those in Fig. 3, as a result of the

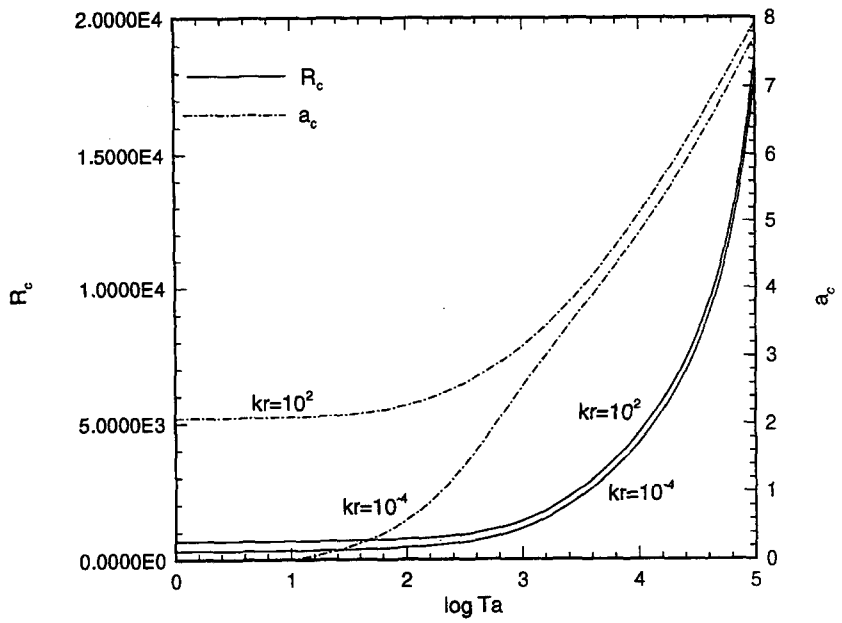

Fig. 3. The critical Rayleigh number R_c and wavenumber a_c as functions of the Taylor number Ta for various values of the thermal conductivity ratio k_r with $Bi = 0$ and $d_r = 10$ and $M = 0$.

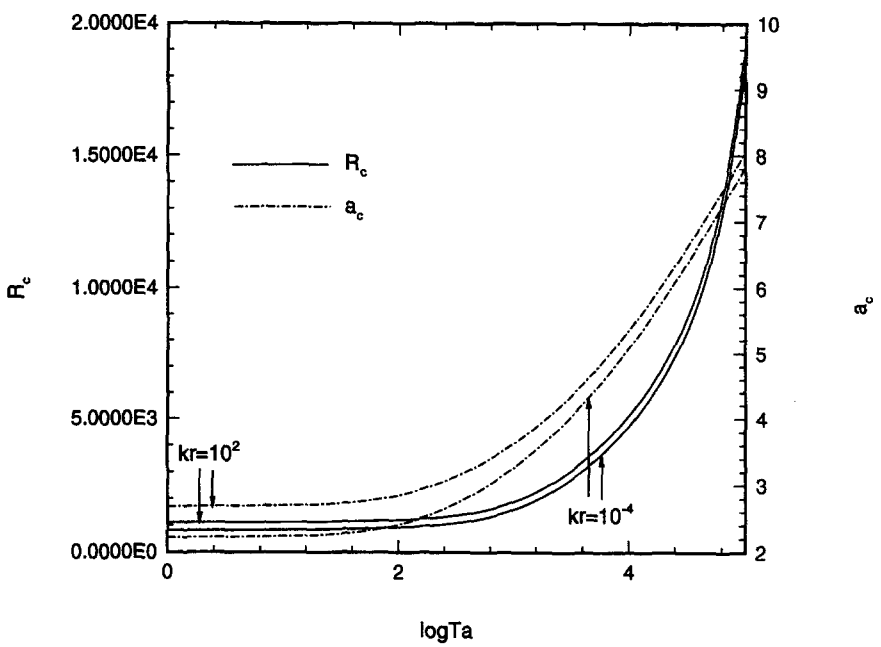

Fig. 4. The critical Rayleigh number R_c and wavenumber a_c as functions of the Taylor number Ta for various values of the thermal conductivity ratio k_r with $Bi^{-1} = 0$, $d_r = 10$ and $M = 0$.

thermal condition depicted previously. The critical Rayleigh number R_c and wavenumber a_c increase with the Taylor number Ta insignificantly for $Ta < 10^3$ and vary rapidly for $Ta > 10^4$. As discussed previously, the effect of the thermal conductivity ratio d_r suppresses the onset of convection and increases the critical Rayleigh number. From Fig. 4, it can be seen that the parallel flow does not exist for cases with the constant temperature condition.

In considering the pure Marangoni convection, the Rayleigh number R is set to zero. Figure 5 shows the critical Marangoni number M_c and wavenumber a_c as functions of the Taylor number Ta for various values of the thermal conductivity ratio k_r and for the case of constant heat flux at the upper surface with $Bi = 0$ and $d_r = 10$ and $R = 0$. In the absence of the buoyancy effect, the onset of Marangoni convection is dominated by the surface tension effect. For the limiting case, constant heat flux at the upper surface and constant temperature at the fluid-solid boundary, Kad-

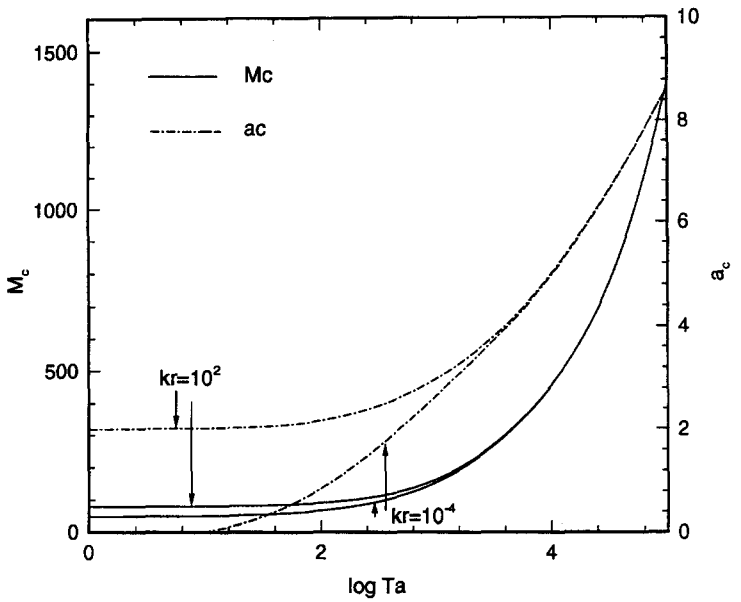

Fig. 5. The critical Marangoni number M_c and wavenumber a_c as functions of the Taylor number Ta for various values of the thermal conductivity ratio k_r with $Bi = 0$, $d_r = 10$ and $R = 0$.

dame and Lebon [15] have shown that the effect of Coriolis force upon the critical condition $[M_c, a_c]$ gives rise to [329.4, 4.26] for $Ta = 5 \times 10^3$ and [457.5.01] for $Ta = 10^4$, provided $C = 10^{-5}$. The comparable calculations in this study are [329.493, 4.256] for $Ta = 5 \times 10^3$ and [456.962, 5.007] for $Ta = 10^4$. The system is situated in a more stabilizing state under the effect of Coriolis force and, the critical Marangoni number M_c and wavenumber a_c increase with the Taylor number Ta, significantly for $Ta > 10^4$. For a large enough Taylor number Ta the critical Marangoni number M_c and wavenumber a_c become independent of k_r; this manifestation illustrates the prevailing effect of Coriolis force over the thermal effect. The thermal conductivity ratio k_r would also stabilize the system in the Marangoni convection, as it would act in the thermal convection. The parallel flow is possible only when the Taylor number Ta is small and the thermal conductivity ratio k_r is tiny. For $Ta = 0$, a vanishing critical wavenumber with M_c being 48 is presented for the parallel flow [17]. Figure 5 also shows that the valid range of the Taylor number Ta for the parallel flow is, for $k_r = 10^{-4}$, about 0–10.

Figure 6 shows the critical Marangoni number M_c and wavenumber a_c as functions of the Taylor number Ta for various values of the thermal conductivity ratio k_r with $Bi = 10$, $d_r = 10$ and $R = 0$. The combined effect of constant temperature and constant heat flux is taken into account. As mentioned in ref. [7], when the free surface is a good conductor, any thermal variation across the surface decays rapidly and results in a small surface tension traction. Comparing the case of $Bi = 10$ in Fig. 6 with that of $Bi = 0$ in Fig. 5, for the large Biot number Bi, the free surface deviates from being a good conductor and the critical Marangoni number M_c increases with the Biot number Bi. The critical wavenumber a_c also has this kind of increasing trend. The significant difference between Fig. 5 and Fig. 6 is that, for small values of the Taylor number Ta, the increase of the critical wavenumber a_c with the thermal conductivity ratio k_r is rapid for $Bi = 0$ and slow for $Bi = 10$. In other words, for small values of the Taylor number Ta, the increase of the critical wavenumber a_c with the Biot number Bi is rapid for $k_r = 10^{-4}$ and slow for $k_r = 10^2$. Without the rotation $Ta = 0$, the critical conditions $[M_c, a_c]$, corresponding to $k_r = 10^{-4}$ and 10^2, respectively, are [48.048, 0.007] and [79.421, 1.987], provided $Bi = 0$, and are [383.15, 2.451] and [413.13, 2.740], provided $Bi = 10$. The conclusions agree very well with previous works [7, 17]. When $Ta \geqslant 2.5 \times 10^4$, as before, the critical condition $[M_c, a_c]$ becomes independent of the thermal conductivity ratio k_r.

For the Bénard–Marangoni convection, the role of the solid plate thickness seems to be minor, unless the fluid layer is comparably thick. Figure 7 shows the locus of the critical Marangoni number M_c and Rayleigh number R_c for various values of the Taylor number Ta and thermal conductivity ratio k_r and for the case of constant heat flux at the upper free surface with $Bi = 0$ and $d_r = 10$. Increasing the Taylor number Ta or the thermal conductivity ratio k_r as well as decreasing the Marangoni number M would stabilize the system and increase the critical Rayleigh number R_c. For fixed values of the Rayleigh number R, the critical Marangoni number M_c increases with the thermal conductivity ratio k_r. For pure Marangoni convection without rotation, $R = 0$ and $Ta = 0$, the critical conditions $[M_c, a_c]$ are [48.048, 0.007], [55.125, 0.987] and [79.420, 1.987] for $k_r = 10^{-4}$, 10^{-1} and 10^2, respec-

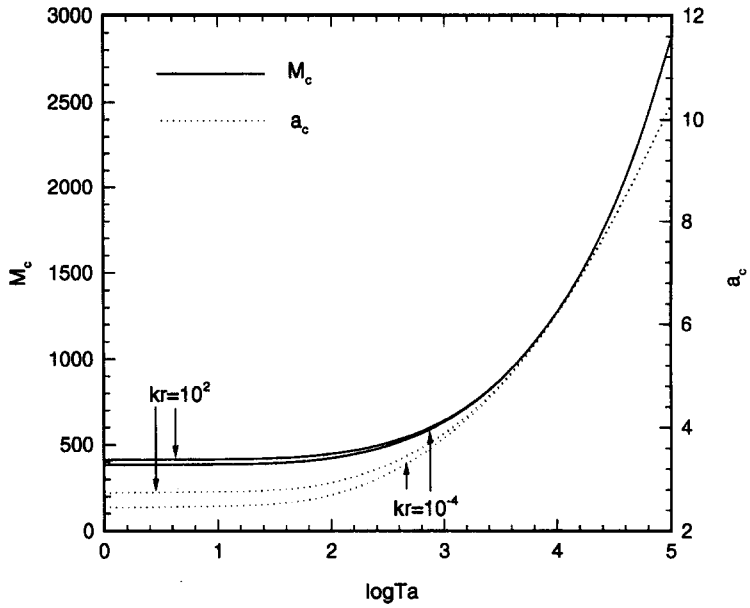

Fig. 6. The critical Marangoni number M_c and wavenumber a_c as functions of the Taylor number Ta for various values of the thermal conductivity ratio k_r with $Bi = 10$, $d_r = 10$ and $R = 0$.

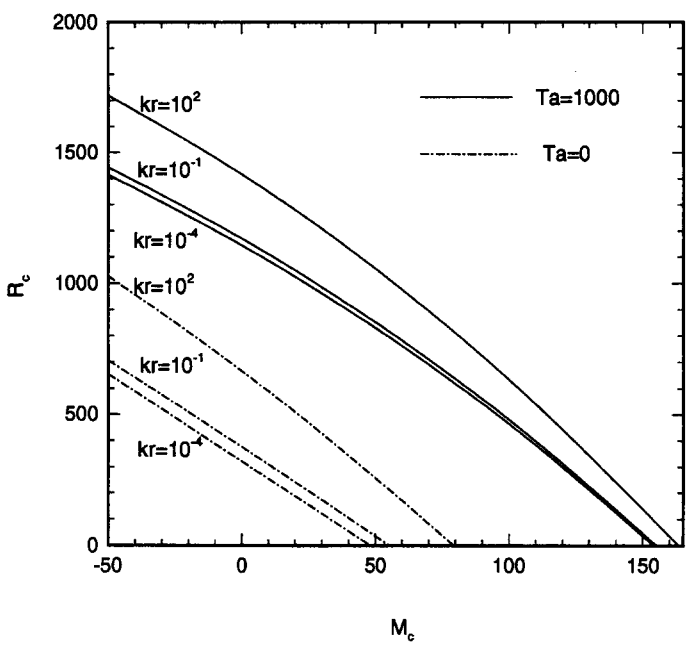

Fig. 7. The locus of the critical Marangoni number M_c and Rayleigh number R_c for various values of the Taylor number Ta and thermal conductivity ratio k_r with $Bi = 0$ and $d_r = 10$.

tively [17]. While with rotation, $Ta = 10^3$, the critical conditions $[M_c, a_c]$ are [154.076, 2.645], [155.070, 2.686] and [163.317, 2.971] for $k_r = 10^{-4}$, 10^{-1} and 10^2, respectively. For pure Bénard–Rayleigh convection without rotation, $M = 0$ and $Ta = 0$, the critical condition $[R_c, a_c]$ is [320.407, 0.007], [375.881, 0.827] and [666.326, 2.077] for $k_r = 10^{-4}$, 10^{-1} and 10^2, respectively. While with rotation, $Ta = 10^3$, the critical condition $[R_c, a_c]$ is [1145.334, 2.539], [1171.162, 2.613] and [1416.445, 3.142] for $k_r = 10^{-4}$, 10^{-1} and 10^2, respectively. For $M < 0$, the surface tension increases with the temperature and the stability of the system is strengthened, while, for $M > 0$, the surface tension decreases with the temperature and the stability of the system is weakened. The decreasing of the critical Rayleigh number R_c with the Marangoni number M is illustrated. The parallel flow assumption is valid for small values of the Taylor number Ta and

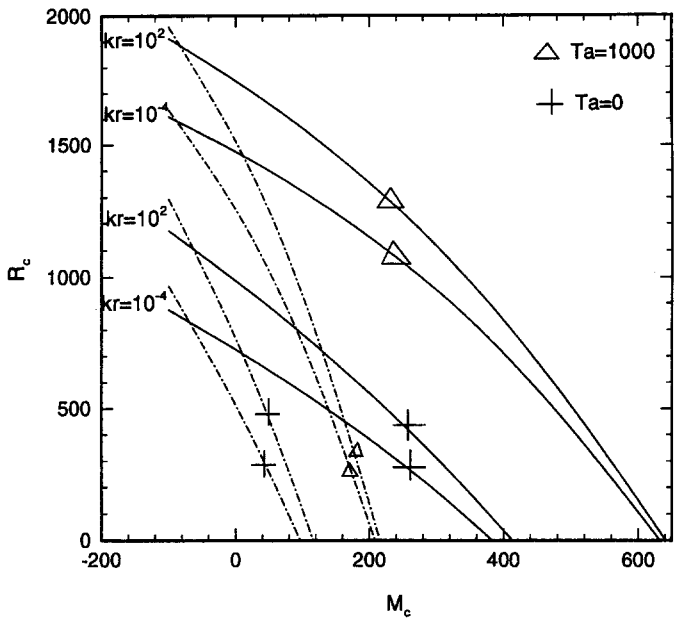

Fig. 8. The locus of the critical Marangoni number M_c and Rayleigh number R_c for various values of the Taylor number Ta and thermal conductivity ratio k_r with $Bi = 1$ (dashed line) and $Bi = 10$ (solid line) and $d_r = 10$.

the parameter $k_r d_r$. For the case $k_r d_r = 10^{-3}$, $R = 0$ and $M = 48.048$ as well as $M = 0$ and $R = 320.407$ would fit the following parallel flow solution [17],

$$R/320 + M/48 = 1 + k_r d_r.$$

Figure 8 shows the locus of the critical Marangoni number M_c and Rayleigh number R_c for various values of the Taylor number Ta and thermal conductivity ratio k_r with $Bi = 1$ and 10 and $d_r = 10$. Increasing the thermal conductivity ratio k_r, the Taylor number Ta or the Biot number Bi as well as decreasing the Marangoni number M does suppress the onset of convection and increase the critical Rayleigh number R_c, provided $M \geqslant 0$.

For the region of the Marangoni number M being negative, the surface tension increases with the temperature and an insulated upper surface would intensify the stability of the system. A higher Biot number Bi would result in the decreasing of the critical Rayleigh number R_c. With the rotation $Ta = 10^3$, the critical conditions $[M_c, a_c]$ corresponding to $k_r = 10^{-4}$ and 10^2, respectively, are: [154.076, 2.645] and [163.317, 2.971], provided $Bi = 0$ and are [632.196, 3.790] and [640.752, 3.881], provided $Bi = 10$. For $k_r \to \infty$ and $Bi = 0$, approximate and comparable results are [164, 3.0] for $Ta = 10^3$ [12] and [457. 5.01], provided $C = 10^{-5}$, for $Ta = 10^4$ [15].

The parallel flow is associated with the vanishing wavenumber a. It requires that the boundaries be fixed with the uniform heat flux such that the parallel flow assumption becomes realistic—this is achieved only when the parameter $k_r d_r$ is small enough or zero. The approximate parallel flow solution has been derived for a two layer solid–fluid system, multi-solid-fluid system and a two layer fluid–fluid system [17–19]. The critical Rayleigh number R_c and wavenumber a_c, as functions of the parameter $k_r d_r$ for various values of the thickness ratio d_r and Taylor number Ta for the case of constant heat flux at the upper free surface with $Bi = 0$ and $M = 0$, are shown in Fig. 9 and Fig. 10, respectively. The parallel flow solution is valid only for small values of the Taylor number. It is noticed that, for $d_r = 10^{-1}$ and 1, the onset motion is 'parallel' up to $k_r d_r = 0.4$ and 0.18, respectively, for $Ta = 0$, while, for small values of the Taylor number, e.g. $Ta = 10$, the 'parallel' motion is up to $k_r d_r = 0.35$ and 0.16, respectively. Even for finite, but small, values of wavenumber, the critical Rayleigh number calculated from the parallel flow solution is still accurate up to $a_c = 0.6$–0.9, when $Ta = 0$–10 for $d_r = 0.1$–1, respectively.

CONCLUSIONS

The onset of Bénard–Marangoni convective instability of a rotating system, composed of a fluid layer and a solid plate, is studied numerically. Parts of the present results are coincident with previous investigations. It is shown that the effect of the Coriolis force suppresses the onset of convection and hence stabilizes the system. Variations of critical conditions are obscure for small values of the Taylor number Ta and significant for large values of the Taylor number Ta. In general, for higher values of the thermal conductivity ratio k_r, thickness ratio d_r, Biot number Bi and Taylor number Ta could lead to a larger critical Rayleigh number or Marangoni number, as a result of their stabilizing factors. When the solid plate is

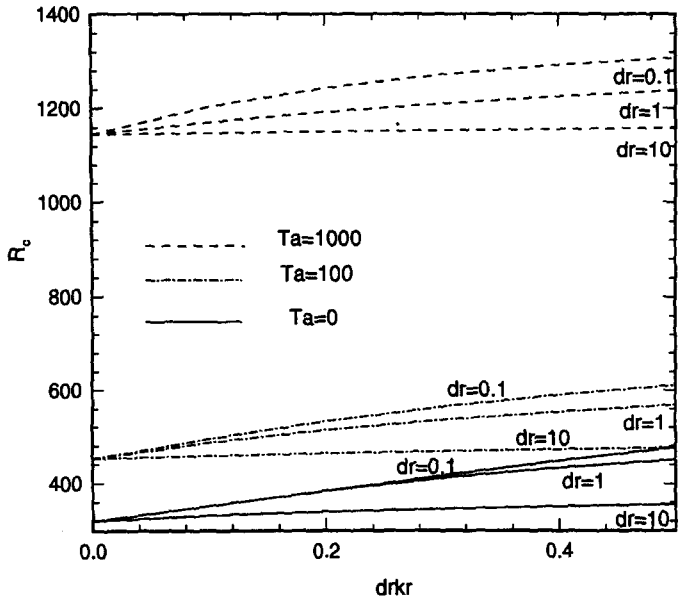

Fig. 9. The critical Rayleigh number R_c as a function of the parameter $k_r d_r$ for various values of the depth ratio d_r and Taylor number Ta with $Bi = 0$ and $M = 0$.

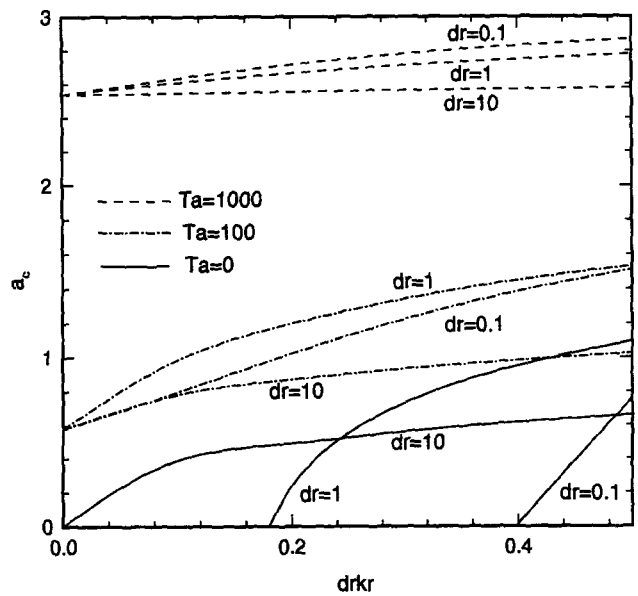

Fig. 10. The critical wavenumber a_c, as a function of the parameter $k_r d_r$ for various values of the depth ratio d_r and Taylor number Ta with $Bi = 0$ and $M = 0$.

relatively thin or poorly conductive, the parallel flow solution remains valid for small values of the Taylor number Ta.

REFERENCES

1. Pearson, J. R. A., On convection cells induced by surface tension. *Journal of Fluid Mechanics*, 1958, **4**, 489–500.
2. Pellow, A. and Southwell, R. V., On maintained convective motion in a fluid heated from bellow. *Proceedings of the Royal Society, London*, 1940, **176**, 312–343.
3. Chandrasekhar, S., *Hydrodynamic and Hydromagnetic Stability*. Oxford University Press, London, 1961.
4. Sparrow, E. M., Goldstein, R. J. and Jonsson, V. K., Thermal instability in a horizontal fluid layer: effects of boundary conditions and nonlinear temperature. *Journal of Fluid Mechanics*, 1964, **18**, 513–528.
5. Veronis, G., Large-amplitude Bénard convection in a rotating fluid. *Journal of Fluid Mechanics*, 1968, **31**, 113–139.
6. Rossby, H. T., A study of Bénard convection with and without rotation. *Journal of Fluid Mechanics*, 1969, **36**, 309–335.
7. Nield, D. A., Surface tension and buoyancy effects in cellular convection. *Journal of Fluid Mechanics*, 1964, **19**, 341–352.
8. Davis, S. H. and Homsy, G. M., Energy stability theory

for free-surface problems: buoyancy-thermocapillary layers. *Journal of Fluid Mechanics*, 1980, **98,** 527–533.
9. Pérez-Garcia, C. and Carneiro, G., Linear stability analysis of Bénard–Marangoni convection in fluids with a deformable free surface. *Physics of Fluids*, 1991, **3,** 292–298.
10. Ferm, E. N. and Wollkind, D. J., Onset of Rayleigh–Bénard–Marangoni instability: comparison between theory and experimentals. *Journal of Non-equilibrated Thermodynamics*, 1982, **9,** 169–170.
11. Koschmieder, E. L. and Biggerstaff, M. I., Onset of surface tension driven Bénard convection. *Journal of Fluid Mechanics*, 1986, **167,** 49–64.
12. Vidal, A. and Acrivos, A., The influence of Coriolis force on surface-tension-driven convection. *Journal of Fluid Mechanics* 1966, **26,** 807–818.
13. McConaghy, G. A. and Finlayson, B. A., Surface tension driven oscillatory instability in a rotating fluid layer. *Journal of Fluid Mechanics*, 1969, **39,** 49–55.
14. Friedrich, R. and Rudraiah, N., Marangoni convection in a rotating fluid layer with non-uniform temperature gradient. *International Journal of Heat Mass and Transfer* 1984, **27,** 443–449.
15. Kaddame, A. and Lebon, G., Bénard–Marangoni convection in a rotating fluid with and without surface deformation. *Applied Scientific Research*, 1994, **52,** 295–308.
16. Nield, N. A., Onset of convection in a fluid layer overlying a layer of a porous medium. *Journal of Fluid Mechanics*, 1977, **81,** 513–522.
17. Yang, H. Q., Boundary effects on the Bénard–Marangoni instability. *International Journal of Heat and Mass Transfer*, 1992, **35,** 2413–2420.
18. Yang, H. Q., Thermal instability and heat transfer in a multi-layer system subjected to uniform heat flux from below. *International Journal of Heat and Mass Transfer*, 1991, **34,** 1701–1715.
19. Yang, H. Q. and Yang, K. T., Bénard–Marangoni instability in two layer system with uniform heat flux. *Journal of Thermophysics*, 1990, **4,** 73–78.
20. Vidal, A. and Acrivos, A., Nature of the natural state in surface tension driven convection. *Physics of Fluids* 1966, **9,** 619.
21. Garcia-Ybarra, P. L., Castillo, J. L. and Velarde, M. G., Bénard–Marangoni convection with a deformable interface and poorly conducting boundaries. *Physics of Fluids*, 1987, **30,** 2655–2661.